Deep learning Convolution Neural Networks Pulmonary Tuberculosis Detection

Mr. Athukuri Prasad
Scholar, JJTU
mailsofprasad@gmail.com
of ECE

Dr. Alok Agarwal
Internal Guide
alokagarwal26aaa@gmail.com
Dept. of ECE

Dr.Ch. Rami Reddy Research
Co - Guide
crreddy229@gmail.com Dept.
Dept. of EEE

Abstract. Pulmonary Tuberculosis (TB), one of the transmissible diseases, is one of the top 10 causes of mortality in the world, accounting for one-tenth of all deaths. It is necessary to improve the treatment and screening of tuberculosis patients in TB-affected nations. An extensive systematic evaluation of deep learning-based computer-aided diagnostic (CAD) systems that are used to analyse chest X-rays for the purpose of detecting pulmonary tuberculosis is presented in this work (TB). Deep learning has lately risen to the top of the list of most effective approaches, notably in the field of image analysis, which includes medical imaging. Convolutional Neural Networks (CNNs) are commonly utilised for tuberculosis diagnosis in deep learning applications. A CNN model is often composed of convolutional layers, sub-sampling/pooling layers, and fully connected layers, with the convolutional layers being the most frequent. In addition, this work provides a detailed assessment of CNN models for the diagnosis of tuberculosis. The advancement of computer-aided diagnostic (CAD) systems has resulted in a reduction in the time it takes to diagnose tuberculosis (TB).

Keywords: Tuberculosis, Convolution Neural Networks, Data set, Histogram.

1. Introduction

In order to enhance tuberculosis (TB) diagnosis during the screening process, researchers have been developing computer-aided diagnostic (CAD) systems since the 1970s. Radiology assistant devices (CADs) are equipped with an autonomous diagnostic system that may be utilised in distant locations to assist radiologists [1]. Over the last several years, advances in the science and methods of artificial intelligence (AI) have resulted in substantial advancements in the field of automated computer picture identification. [2] [3] CAD systems employed artificial intelligence to analyse radiological pictures in order to diagnose anomalies and alleviate the scarcity of radiologists, which was particularly acute in poor nations. Alzheimer's disease [4], breast cancer, prostate cancer, lung cancer [5], neurological disorders (e.g. bone suppression), and skin lesions (e.g. skin lesions) are among the diseases for which CAD systems are frequently utilised in the interpretation of medical pictures [7]. [8] Machine Learning (ML) and Deep Learning (DL) are two of the most extensively utilised artificial intelligence technologies for developing CAD systems that can analyse chest X-ray CXRs. The proliferation of medical image data as a result of advancements in science and technology, as well as the proliferation of medical imaging modalities, has made the analysis and interpretation of medical image data for radiologists more

complex. [9] When bacteriological tests fail to produce a suitable result, radiography is called upon to assist in the diagnosis. Mycobacterium tuberculosis is a bacteria that is responsible for tuberculosis. Active TB is characterised by symptoms such as fever, cough, night sweats, chest discomfort, weight loss, weariness, and anorexia, among others. The World Health Organization (WHO) recommends high-quality chest X-ray (CXR) pictures and laboratory-based diagnostic tests to be utilised for early diagnosis of tuberculosis (TB) and to close the tuberculosis (TB) detection gap. The majority of persons who have symptoms of tuberculosis are tested by evaluating their CXR using a CAD system.WHO states that CXR is an effective method for systematic screening of patients with symptoms of tuberculosis and for identifying those who need microscopic examination of their sputum. The first step in diagnosing unexplained cough is to get a CXR posteroanterior (PA) picture of the lung. Although the lungs are the most usually afflicted organ system in the body when it comes to chest illness, tuberculosis (TB) may affect any organ system in the body. [10]. In chest radiography, CAD systems may identify a variety of disorders such as pulmonary consolidation, pneumothorax, pleural effusion, cardiac hypertrophy, nodules, infiltration, atelectasis, and emphysema, among others. The anatomical anatomy of the chest is seen in Figure 1.

(a)   (b)   (c)
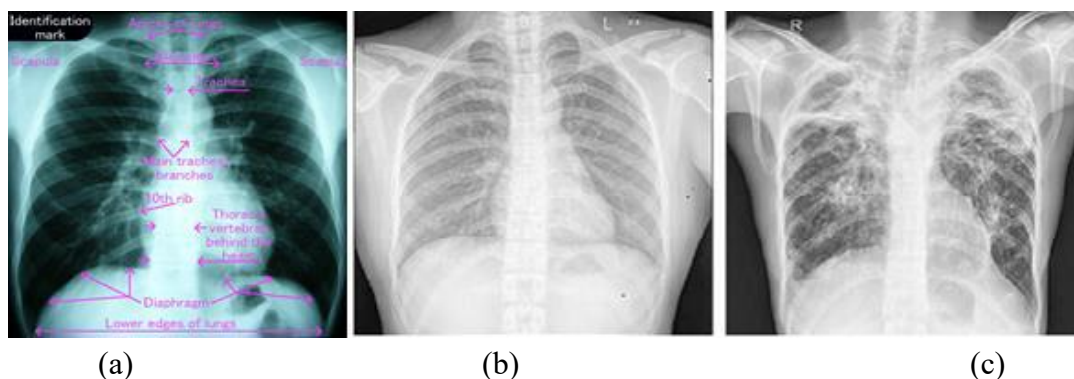
Figure 1. Chest X-ray image a) Chest anatomy b) A healthy chest X-ray image c) Tuberculosis with multiple cavitation's X-ray images.

2. Deep learning

Deep learning is a relatively new and rapidly expanding discipline that provides good solutions to a wide range of CAD jobs. Deep learning has swiftly gained popularity in the area of Radiology [11], and it is expected to continue to do so. Specifically, the development of Deep Convolutional Neural Networks (CNNs) has played a critical role in the extraction of features for tuberculosis illness diagnosis and the categorization of chest X-ray pictures as normal or abnormal, among other applications. Specifically, the CNN design is comprised of three primary layers: convolutional, pooling, and fully connected layers (FC). In most cases, the pooling layer is used in conjunction with the convolution layer to reduce the feature map size. According to the figure 2, the maximum pooling and the average pooling functions are the two most often utilised types of pooling functions. When using maximum pooling, the biggest element (for example,

2X2) is chosen from the window, but when using average pooling, the average of all elements is chosen. Overfitting is avoided by limiting the amount of network parameters and computations performed by the pooling layer as well. FC layers are used to encode the whole amount of information included in the input picture. When working with an input picture, the FC layer's goal is to categorise it into different categories using the characteristics acquired from the preceding layers. Softmax and other activation functions are utilised after the FC layer in order to get the final result.
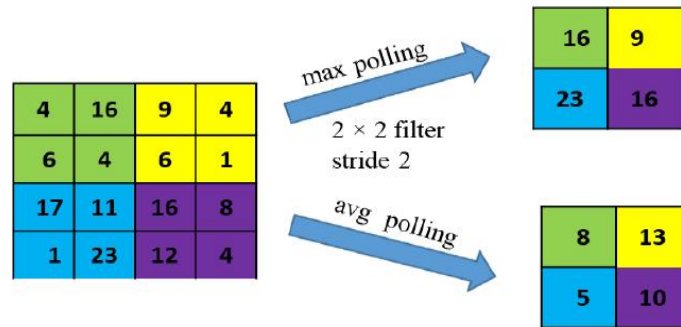

Figure 2. Illustration of max pooling and average pooling

ImageNet is a high-quality visual data collection that comprises more than 15 million high-resolution photographs covering nearly 22,000 categories. ImageNet is a visual data collection that contains more than 15 million high-resolution photos representing nearly 22,000 categories. ImageNet is a high-quality visual data collection that comprises more than 15 million high-resolution photos across approximately 22,000 categories. ImageNet is a part of the National Institutes of Health. The ImageNet dataset is often used by academics to test their picture classification algorithms on vast volumes of data, and it is available for free online. The ImageNet Large Scale Visual Recognition Challenge (ILSVRC) tests visual recognition capabilities by using a smaller subset of the ImageNet, which consists of just 1000 categories, in order to assess their abilities. The effective use of deep learning algorithms on the ImageNet challenge from 2012 is shown in Figure 3.
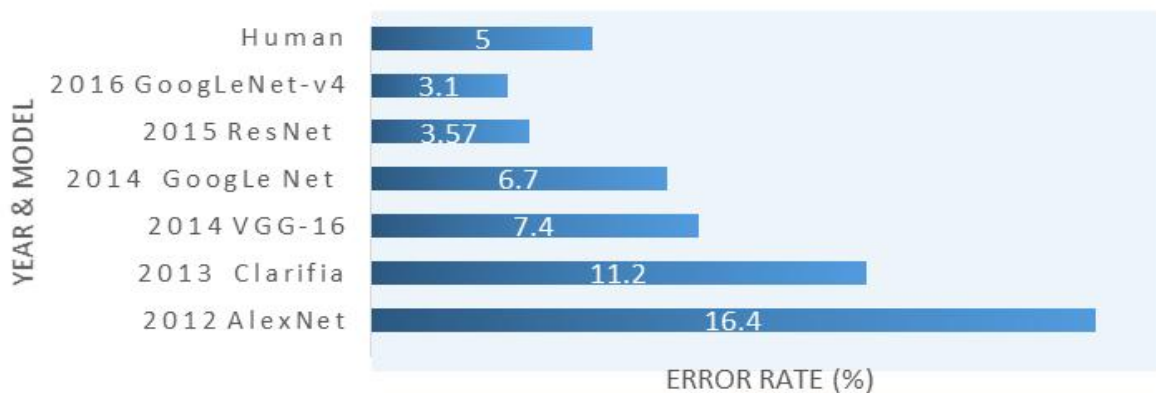
**Figure 3**. Accuracy of various DL models for the ImageNet challenge

CNNs have risen in popularity in recent years, owing to the birth of new kinds of networks and the introduction of sophisticated graphics processing units (GPUs). The training of deeper and more intricate convolutional networks has been possible because to the advancement of computational resources [18]. There have been several variants on CNNs suggested, including LeNet [12], AlexNet [13], VGGNet [14], GoogleNet [15], ResNet [16], DenseNet [17], and R-CNN, among others. Figure 4 depicts a simple CNN architecture for TB classification using LeNet [26], as implemented in LeNet [27]. Convolutional layers, sub-sampling/pooling layers, and fully linked layers have all been used in the past to construct it. AlexNet, as suggested by Krizhevsky et al. [13], is a deep convolutional neural network constructed of five convolutional and three fully-connected layers, with three convolutional layers on top of each other. In AlexNet, the sigmoid activation function was replaced with a ReLU activation function in order to make model training more straightforward. The VGG-16 [14] was developed by K. Simonyan and A. Zisserman and consists of 13 convolutional layers and three fully-connected layers. The Visual Geometric Group (VGG) research group has developed a series of convolution network models, beginning with VGG-11, VGG-13, VGG-16, and VGG-19, all of which are based on the visual geometry.
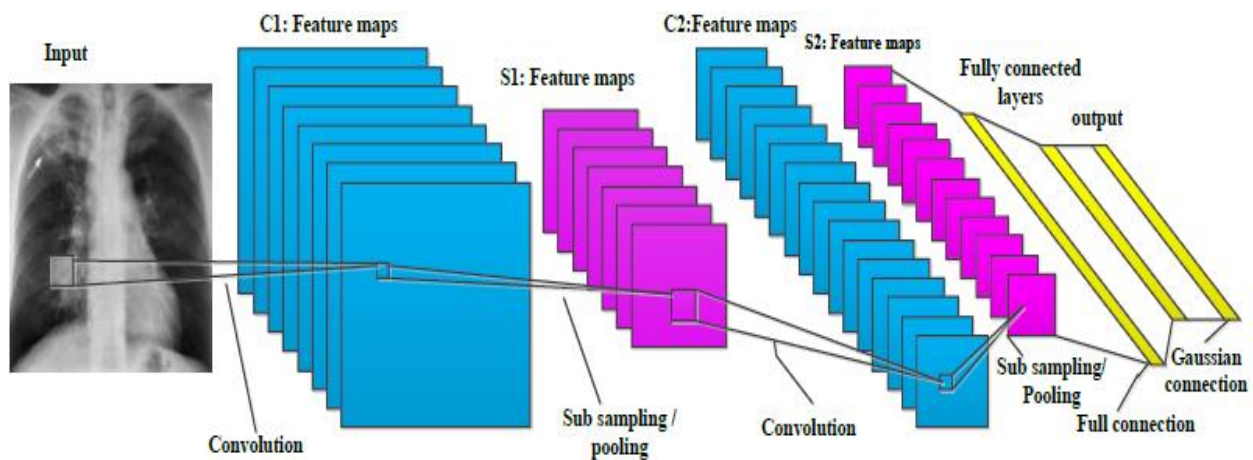

Figure. 4. A basic CNN architecture using LeNet [19].

The primary goal of the VGG group is to better understand how the depth of convolutional networks influences the accuracy of image classification and recognition models in order to improve their accuracy. When compared to the maximum VGG19, which has 16 convolutional layers and 3 fully connected layers, the lowest VGG11 has 8 convolutional layers and 3 fully connected layers, which is much less. The last three completely linked layers are the same as those seen in the different VGG versions. Szegedy and colleagues [15] GoogleNet is a proposed image categorization network that consists of 22 distinct layers and is comprised of 22 different layers. The inclusion of conception layers is the basic concept underlying the GoogleNet project. Each inception layer convolves the input layers in a parallel manner, utilising a different filter

size for each layer inception. The ResNet design, suggested by Kaiming He et al. [16], consists of 33 convolutional layers and one fully-connected layer, with one fully-connected layer at the top. The notion of employing several hidden layers and very deep neural networks was presented by many models, however it was later discovered that such models were plagued by the issue of the disappearing or expanding gradients problem. It is necessary to create skip layers (shortcut connections) in order to eliminate the issue of disappearing gradients. In the work of Gao et al. [17], they created a DenseNet that is composed of many dense blocks and transition blocks that are inserted between two neighbouring dense blocks. There are three stages of batch normalisation before a ReLU and a three-way convolution operation are performed on the data in the dense block. Batch Normalization, 1x1 Convolution, and average Pooling are used as transition blocks in the algorithm. Comparing CNNs to the most advanced handmade feature detectors available, CNNs are an efficient approach for identifying features of an object and obtaining high classification performance. In order to overcome overfitting concerns while training CNN, a large quantity of data is necessary. The transfer of learning is a solution in the medical area since comprehensive data is not accessible in this domain. It is common practise to use two transfer learning strategies, which are as follows: I a pre-trained CNN model used as a feature extractor, and (ii) fine tuning a pre-trained CNN model using data from the associated domain.
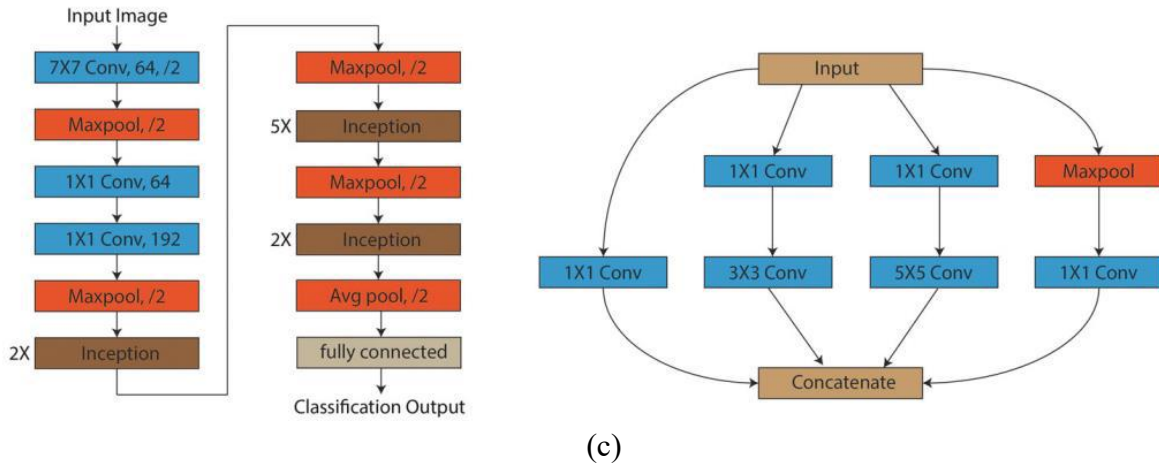

(a)

(b)

(c)
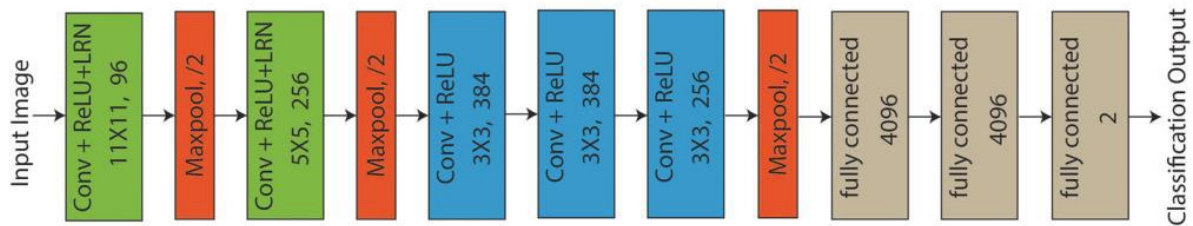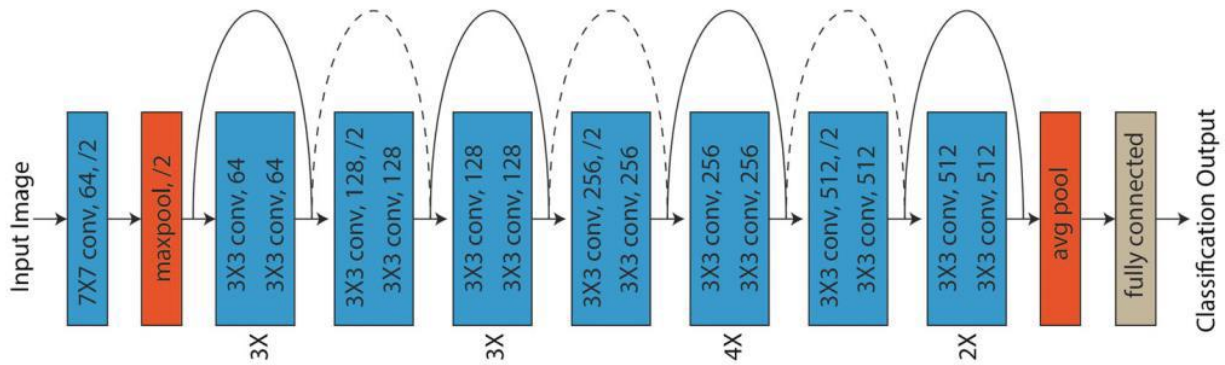
Figure 5 (a) AlexNet Architecture (b) ResNet Architecture (c) GoogleNet Architecture

3. DATASET

Because of privacy limitations enforced by academic and research organisations, many researchers have refrained from publishing data on tuberculosis categorization in the CXRs, which includes some publicly accessible datasets. The following is a high-level summary of the datasets.

3.1. Tuberculosis X-ray (TBX11K)

TBC11K is a collection of 11200 radiographs, containing 1200 photos showing evidence of tuberculosis symptoms, 5000 ill but not tuberculosis images, and 5000 healthy images. [21] All X-ray pictures have a resolution of 3000 x 3000 pixels.

3.2. JSRT dataset

The X-ray pictures in this Montgomery dataset were obtained from the TB preventive programme of Montgomery County, in the United States. This dataset comprises 80 X-ray pictures that are considered normal, and 58 X-ray images that are considered Tuberculosis symptoms, respectively. The X-rays have a resolution of either 4,020 x 4,892 pixels or 4,892 x 4,020 pixels [23].

3.3 Mantgomery dataset (MC)

The X-ray pictures in this Montgomery dataset were obtained from the TB preventive programme of Montgomery County, in the United States. This dataset comprises 80 X-ray pictures that are considered normal, and 58 X-ray images that are considered Tuberculosis symptoms, respectively. The X-rays have a resolution of either 4,020 x 4,892 pixels or 4,892 x 4,020 pixels [23].

3.4. Shenzhen dataset (CH)

Photographs taken by the Shenzhen No.3 Hospital in the Chinese city of Shenzhen are included in this data collection. There are 326 normal X-ray pictures of TB and 336 abnormal X-ray photos of tuberculosis in this collection. The ×-ray pictures have a resolution of 3,000 x 3,000 pixels, which is a high quality [23].

3.5. India dataset (IN)

[Were obtained from two separate X-ray machines at the National Institute for Tuberculosis and Respiratory Diseases, New Delhi, and were suggested by Chauhan et al. [24] as two distinct datasets. It was divided into two parts: a training set (52 CXRs without TB and 52 with TB) and a test set (26 CXRs without TB and 26 TB). The training set (50 non-TB CXRs and 50 TB CXRs) and the test set (25 without TB and 25 TB CXRs) were both included in the DB in exactly the same way [24].

3.6. Belarus Dataset

The X-ray pictures and chest CT scans of 420 tuberculosis patients were used to create this dataset. The CXR images have a spatial resolution of 2248 x 2248 pixels, which is a high level of detail. The information was generated by a number of institutions affiliated with the Ministry of Health of the Republic of Belarus.

4. Discussion

TB identification from CXR pictures using CNN models is the subject of this work, which surveys and summarises research publications published between 2010 and 2020 on the subject. As a result of its superior performance in the issue of Pattern Recognition, CNNs are often employed in the building of CAD systems today. CNN models outperform traditional statistical approaches in terms of result prediction when compared to the data available from the data. A updated AlexNet and GoogleNet CNN model, built by Liu et al. [19], was used to identify TB symptoms in X-ray pictures. The model's accuracy was found to be 85.68 percent. Hooda et al. [20] present an ensemble of three architectures for TB detection, namely AlexNet, GoogleNet, and ResNet, which they call the AlexNet, GoogleNet, and ResNet ensemble. The ensemble architecture achieves an accuracy of 88.24 percent based on the data. The authors Ban et al. [21] developed deep learning-based Computer-aided TB diagnosis as a new method of diagnosing the disease (CTD). The authors created a new benchmark TB dataset (TBX11K), which comprises 11200 CXR pictures and serves as a baseline for future research. The authors recommended that deep learning models be used to classify X-ray images while also detecting TB areas at the same time. According to Hwang et al. [25], the first deep convolution neural network (CNN) based approach for tuberculosis diagnosis was suggested utilising the modified Alexnet network and transfer learning techniques. Based on the 14-layer CNN architecture and data augmentation approach suggested in this research [26], a TB detection method has been devised. This CNN model accurately classifies CXR pictures from public datasets (MC, CH, and IN) into TB positive and negative classes with an accuracy of 87.29 percent based on TB positivity and negative classes.

Ghorakavi [27] suggested a deep neural network, ResNet18, with the data augmentation procedure being utilised to boost the accuracy of the network's predictions. S. J. Heo and colleagues [28] It is suggested to use D-CNN, which is a mix of Image CNN (I-CNN) plus demographic parameters such as age, height, weight, and gender to improve classification accuracy. D-CNNs may be used to predict tuberculosis from chest X-rays, and demographic data can be used to improve the accuracy of tuberculosis diagnosis. The accuracy of D-CNN is higher than that of I-CNN. Lakhani and Sundaram [29] recommended that the AlexNet and GoogleNet designs be integrated for the purpose of detecting tuberculosis. It has been shown by Nguyen et al. [30] that the weights of ImageNet are inadequate for TB identification via transfer learning, and that the use of relevant pre-training data is required. In a recent study, Sivaramakrishnan et al. [31] assessed the performance of five pre-trained DL models for TB identification in CXRs. In their research, they discovered that the performance of pre-trained DL models is superior than that of the customised model. CAD software, CAD4TB, is a commercially available programme for the diagnosis of tuberculosis. For the diagnosis of PTB, the authors conducted a systematic analysis of the diagnostic accuracy of CAD software in comparison to a microbiological reference test in the publication [37]. The CAD4TBv6 programme was created using Deep Learning methods, which are described in detail below. The CAD4TBv6 programme has a high sensitivity, with an area under the curve ranging from 0.71 to 0.84 on the sensitivity test. A study published in [38] investigated the performance of three Deep Learning (DL)-based systems, CAD4TB, qXR, and Lunit INSIGHT, for the detection of tuberculosis-associated anomalies in chest X-ray images. The three DL systems were reviewed by the authors in a comparative manner. It is comprised of the CAD4TB (V.6) and qXR (v.2) produced by Qure.ai, as well as Lunit INSIGHT (V 4.7.2) for the Chest X-ray image developed by Lunit, and CAD4TB (V.6) for the CAD4TB (V.6) (South Korea). Lunit and CAD4TB are both capable of reading the DICOM format of CXR images. The result of CAD4TB is shown as an anomaly score ranging from 0 to 100 for tuberculosis detection. qXR and Lunit may detect pulmonary abnormalities such as cavitation, nodule, pneumothorax, and other pulmonary abnormalities from a CXR picture. These three Deep Learning TB are CAD4TB, qXR, and Lunit, as opposed to those who do not.

4. DATASETS AND EXPERIMENTAL SETTINGS

4.1 Datasets Link to main Datasets used:

https://ceb.nlm.nih.gov/repositories/tuberculosis-chest-x-rayimage-data-sets/

Shenzhen Hospital

X-ray Set: X-ray images in this data set have been collected by Shenzhen No.3 Hospital in Shenzhen, Guangdong province, China.

At Shenzhen Hospital, the x-rays were taken as part of the usual treatment provided to the patient. The photographs in this collection are in the JPEG format. It is possible to find 336 normal x-rays and 326 abnormal x-rays displaying different signs of TB within the collection. This data

collection contains X-ray pictures obtained from the TB control programme of the Department of Health and Human Services in Montgomery County, Maryland, in the United States. In this collection, there are 138 posterior-anterior x-rays, of which 80 are normal and 58 are pathological with indications of TB. This collection comprises 138 posterior-anterior x-rays. All pictures are de-identified and made accessible in DICOM format for your convenience. The collection includes a broad variety of anomalies, such as effusions and miliary patterns, among other things.

4.2 Settings

Matlab is the programme that was utilised for the simulation. This product's Image Processing and Neural Network Toolboxes are put to use in this project. The simulations' parameters are as follows: All data is scrambled in such a way that there will never be a repeat sequence of the same data. A small batch of 80 is utilised, with a maximum of 30 Epochs set. Ten percent of all data is used for verification, with a fixed random generator for the first weight selection. A fixed random generator is used for the initial weight selection. This assures that all simulations begin with the same set of random weight values that were previously chosen. As a consequence, there is no deviation in the findings. The usage of this approach is standard throughout all simulations.

5. EVALUATION

The purpose of the assessment is to determine the success rate of two distinct detection techniques. The following strategies are being assessed: picture preprocessing, followed by a hybrid approach, and finally, a hybrid strategy is being tested.

5.1 Various Pre Processing Techniques

After the input data has been improved, the simulation is carried out in real time. Figure 6 depicts the improvement of contrast. The equalisation of histograms is shown in Figures 7 and 8. Figure 9 depicted the final cropped and modified picture that was utilised in the dataset. In the following simulations, several types of picture preprocessing are applied to the input collection of photos to see what happens. Equalization of the histogram, contrast enhancement, reduction of the colour channel, sharpening, and extraction of the trimmed ROI are some of the techniques used.
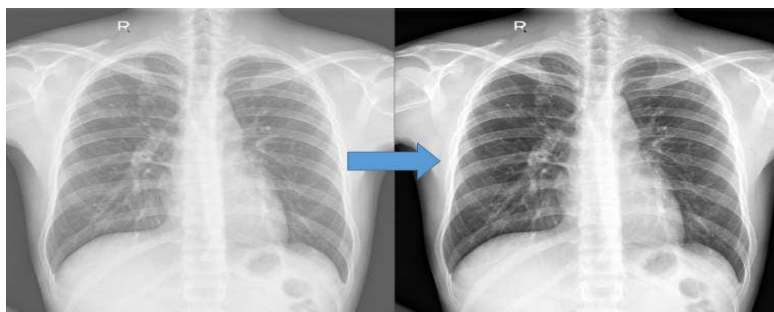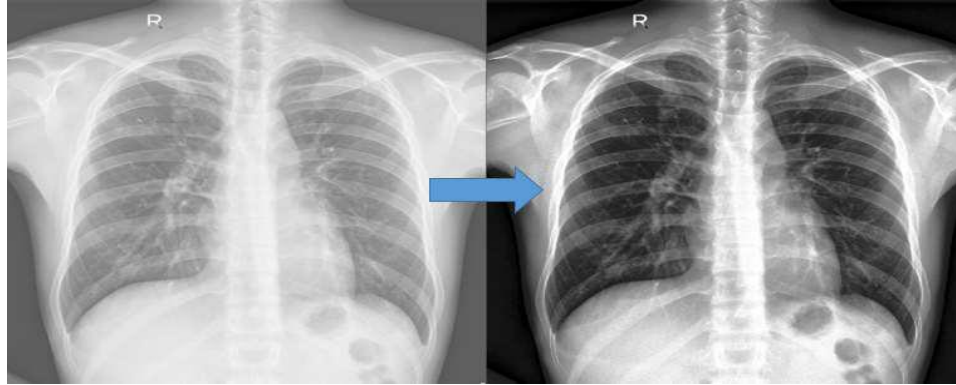

Figure 6. X-ray Contrast Enhancement
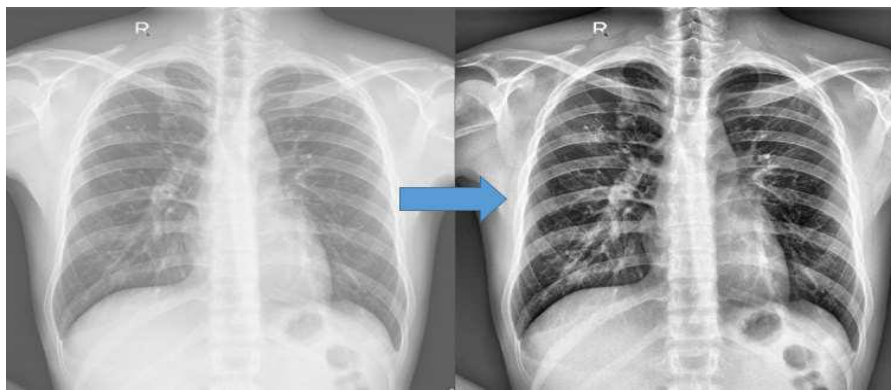
Figure 7. X-Ray Histogram Equalization

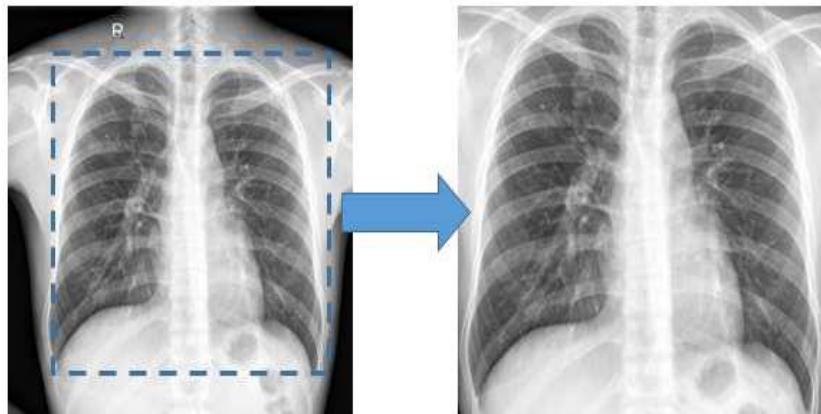Figure 8: X-Ray Adaptive Histogram Equalization

Figure 9: X-Ray Image, Adjusted and Cropped.

Based on Table 1, it can be concluded that the preprocessing strategy that produces the best results is a mix of obtaining a ROI picture of just the lung area and combining it with contrast enhancement. The procedure is repeated three times, with the results recorded in the third accuracy column as 1, 2, and 3. The success percentage here is the highest in the country at 91.04 percent.

7. CONCLUSION

The findings provide strong evidence that picture preprocessing improves accuracy as compared to when images are not preprocessed. With a maximum accuracy of 92.54 percent obtained by extracting simply the ROI from these pictures, the results of the hybrid technique are even better. The key benefit of the hybrid method is that it achieves much greater accuracy by eliminating overfitting. We want to collect additional clinical data in the future, which will allow us to significantly enhance the accuracy of the detection. Collaboration with a third-party entity, such as a state TB hospital, may be used to gather the necessary information for analysis. In the long run, more and more data will be analysed, and the system will continue to learn and increase its precision. Following that, the'system,' or rather the gateway, may be extended to include more institutions while also aiding in the diagnosis of tuberculosis.

References

[1] Hooda R, Mittal A and Sofat S 2018 Tuberculosis Detection from Chest Radiographs : A Comprehensive Survey on Computer-Aided Diagnosis Techniques *Curr. Med. Imaging Rev.* 14 506

[2] Qin C, Yao D, Shi Y and Song Z 2018 Computer-aided detection in chest radiography based on artificial intelligence: A survey *Biomed. Eng. Online* 17 1–23

[3] Raghavendra U, Acharya U R and Adeli H 2019 Artificial Intelligence Techniques for Automated Diagnosis of Neurological Disorders *Eur. Neurol.* 43210 1–24

[4] Adel M, Garali I, Pan X, Fossati C, Gaidon T, Bourennane S and Eric Guedj 2019 Alzheimer's Disease Computer_Aided Diagnosis on Positron Emission Tomography Brain Images using Image Processing Techniques *Computer Methods and Programs in Biomedical Signal and Image Processing* p 13

[5] Firmino M, Angelo G, Morais H, Dantas M R and Valentim R 2016 Computer-aided detection (CADe) and diagnosis (CADx) system for lung cancer with likelihood of malignancy *Biomed. Eng. Online* 15 1–17

[6] Valliani A A A, Ranti D and Oermann E K 2019 Deep Learning and Neurology: A Systematic Review *Neurol. Ther.* 8 351–65

[7] Bakkouri I and Afdel K 2019 Computer-aided diagnosis (CAD) system based on multi-layer feature fusion network for skin lesion recognition in dermoscopy images *Multimed. Tools Appl.* 79 20483–20518

[8] Wernick M, Yang Y, Brankov J, Yourganov G and Strother S 2010 Machine learning in medical imaging *IEEE Signal Process. Mag.* 27 25–38

[9] Nachiappan A C, Rahbar K, Shi X, Guy E S, Eduardo J. Mortani Barbosa J, Shroff G S, Ocazionez D, Schlesinger A E, Katz S I and Hammer M M 2017 Pulmonary Tuberculosis : Role of Radiology in Diagnosis and Management *Radiographics* 37 52–72

[10] Bhalla A S, Goyal A, Guleria R and Gupta A K 2015 Chest tuberculosis : Radiological review and imaging recommendations *Indian J. Radiol. Imaging* 25 213

[11] Yamashita R, Nishio M, Do R K G and Togashi K 2018 Convolutional neural networks: an overview and application in radiology *Insights Imaging* 9 611–29

[12] LeCun Y, Bottou L L, Bengio Y, Ha P and Haffner P 1998 Gradient-based learning applied to document recognition *Proc. IEEE* 86 2278–323

[13] Krizhevsky B A, Sutskever I and Hinton G E 2012 ImageNet Classification with Deep Convolutional Neural Networks *the 25th International Conference on Neural Information Processing Systemsral Information Processing Systems* pp 1097–105

[14] Simonyan K and Zisserman A 2015 Very deep convolutional networks for large-scale imagerecognition *3rd Int. Conf. Learn. Represent. ICLR 2015 - Conf. Track Proc.* 1–14

[15] Szegedy C, Liu W, Jia Y, Sermanet P, Reed S, Anguelov D, Erhan D, Vanhoucke V and Rabinovich A 2015 Going Deeper with Convolutions *The IEEE conference on computer vision and pattern recognition* pp 1–9

[16] He K, Zhang X, Ren S and Sun J 2016 Deep residual learning for image recognition *Proc. IEEE Comput. Soc. Conf. Comput. Vis. Pattern Recognit.* 2016-Decem 770–8

[17] Huang G, Liu Z, Van Der Maaten L and Weinberger K Q 2017 Densely connected convolutional networks *Proc. - 30th IEEE Conf. Comput. Vis. Pattern Recognition, CVPR 2017* 2017-Janua 2261–9

[18] Diamant I, Bar Y, Geva O, Wolf L, Zimmerman G, Lieberman S, Konen E and Greenspan H 2017 Chest Radiograph Pathology Categorization via Transfer Learning *Deep Learning for Medical Image Analysis* (Elsevier Inc.) pp 299–320

[19] Liu C, Cao Y, Alcantara M, Liu B, Brunette M, Peinado J and Curioso W 2018 TX-CNN: Detecting tuberculosis in chest X-ray images using convolutional neural network *Proc. - Int. Conf. Image Process. ICIP* 2017-Septe 2314–8

[20] Hooda R, Mittal A and Sofat S 2019 Automated TB classification using ensemble of deep architectures *Multimed. Tools Appl.* 78 31515–32